Mechanism of lovastatin in promoting ferroptosis of prostate cancer cells by regulating the mevalonate pathway

Yanhong Xiao,[1,2]* Zhengdao Liu,[1]* Yougang Feng,[2] Han Zhu,[1] Bo Wang,[1] Shulian Chen,[1] Guobiao Liang[1]

[1]Department of Urology, Affiliated Hospital of Zunyi Medical University, Zunyi
[2]Department of Urology, Suining Central Hospital, Suining, China

*These authors contributed equally to this work.

ABSTRACT

Prostate cancer (PCa) is a common malignancy in men with limited therapeutic options at advanced stages. Statins, widely prescribed lipid-lowering agents, have demonstrated antitumor activity in PCa, but underlying mechanisms are not fully understood. Studies suggested that tumor progression is facilitated upon activation of mevalonate (MVA) pathway, while it is reduced via MVA pathway inhibition–induced ferroptosis. Therefore, this study aimed to determine whether lovastatin suppresses prostate cancer progression by inducing ferroptosis through inhibition of the MVA pathway. Five clinically used statins were screened in prostate cancer cell lines to identify the most effective compound. Cell proliferation, migration, and invasion were assessed. Ferroptosis was evaluated by measuring intracellular Fe^{2+} and reactive oxygen species (ROS) levels, mitochondrial membrane potential, ferroptosis-related protein expression, and ultrastructural mitochondrial alterations. Rescue experiments were performed using the ferroptosis inhibitor deferoxamine and MVA supplementation. Lovastatin exhibited the strongest inhibitory effect, significantly reducing proliferation, migration, and invasion. Lovastatin significantly suppressing PCa cell aggressiveness and inducing ferroptosis, as evidenced by typical biochemical and morphological markers, all of which were reversed by deferoxamine. MVA supplementation restored cell viability, normalized oxidative stress and iron levels, and reversed alterations in MVA pathway enzymes and ferroptosis-associated proteins. Lovastatin suppresses prostate cancer cell growth and invasiveness by inhibiting the MVA pathway and inducing ferroptosis, highlighting the MVA-ferroptosis axis as a potential therapeutic target for PCa.

Key words: prostate cancer; lovastatin; MVA pathway; ferroptosis.

Correspondence: Prof. Guobiao Liang, Department of Urology, Affiliated Hospital of Zunyi Medical University, No.149 Dalian Road, Huichuan District, Zunyi, Guizhou Province, 563099, China. E-mail: lgb11112021@163.com
Prof. Shulian Chen, Department of Urology, Affiliated Hospital of Zunyi Medical University, No.149 Dalian Road, Huichuan District, Zunyi, Guizhou Province, 563099, China. E-mail: cslzmu@163.com

Conflict of interest: the authors declare no competing interests and all authors confirm accuracy.

Availability of data and materials: the datasets used and analysed during the current study are available from the corresponding author Guobiao Liang on reasonable request.

Funding: this work was supported by the Special Fund for Training outstanding Young Scientific and Technological Talents of Guizhou Province, Grant no. (2015)31.

Introduction

Prostate cancer (PCa) ranks as the fourth most diagnosed cancer worldwide and is the second most prevalent malignancy in men, with over 1.3 million new cases are diagnosed annually, with over 10 million men currently living with PCa. Its mortality rate continues to rise, posing a significant threat to male health and survival.[1-3] Current therapeutic strategies for PCa include radical prostatectomy, radiotherapy, chemotherapy, bone-targeted therapy, poly (ADP-ribose) polymerase-1 (PARP-1) inhibitors, endocrine therapy (e.g., surgical or medical castration), immunotherapy, and palliative care.[4] Given the pivotal role of androgens in PCa initiation and progression, androgen deprivation therapy (ADT) has been widely adopted as a standard treatment.[5] However, most patients develop castration-resistant prostate cancer (CRPC) within two years of ADT, leading to diminished therapeutic efficacy which is a major limitation of ADT.[6] Thus, further elucidating the molecular mechanisms underlying PCa pathogenesis will not only advance preventive and therapeutic approaches but also is crucial for developing precision therapies and improving long-term patient outcomes. Statins, the 3-hydroxy-3-methyl-glutaryl-coenzyme A reductase (HMGCR) inhibitors primarily used for lipid management, have shown demonstrated significant anti-atherosclerotic and cardioprotective effects that establish them as first-line agents for primary and secondary prevention of cardiovascular diseases.[7] Accumulating evidence suggests that statins also possess antitumor properties against hepatocellular carcinoma, esophageal cancer, colorectal cancer, breast cancer, and PCa.[8,9] These effects are mediated through the inhibition of cancer cell proliferation, induction of cell death, and suppression of angiogenesis, often via interference with critical signaling pathways.[8-10] Lovastatin enhances the chemosensitivity of paclitaxel in drug-resistant PCa cells by inhibiting cytochrome oxidase 2C8.[11] Moreover, statins improve chemotherapy resistance in small cell lung cancer by targeting the MVA-geranylgeranyl diphosphate pathway.[12] While statins show therapeutic potential in PCa, the underlying molecular mechanisms remain to be fully elucidated.

The MVA pathway is a central metabolic cascade that supports tumor growth by supplying cholesterol and isoprenoid intermediates essential for cancer cell proliferation and survival.[13,14] In prostate cancer, accumulating evidence has demonstrated that aberrant activation of the MVA pathway is closely associated with tumor progression, and modulating MVA pathway exhibited antitumor effects.[15] The USP35/BRPF1/SREBP2 axis has been identified as a regulator of MVA metabolism in PCa, highlighting MVA pathway as potential therapeutic targets.[16] Dysregulated MVA metabolism further sustains oncogenic signaling, membrane biosynthesis, and therapy resistance, underscoring its pathogenic role in PCa and positioning this pathway as an attractive therapeutic target.[17,18] Recent studies have also revealed a mechanistic link between MVA pathway inhibition and ferroptosis, an iron-dependent form of regulated cell death driven by excessive lipid peroxidation and oxidative stress.[19,20] Ferroptosis is increasingly recognized as a critical vulnerability in prostate cancer, particularly in advanced and castration-resistant disease, where conventional therapies often fail.[21,22] Excessive accumulation of reactive oxygen species (ROS) and disruption of cellular redox homeostasis are key triggers of ferroptosis, leading to mitochondrial dysfunction and irreversible membrane damage.[23] Induction of ferroptosis has been shown to effectively suppress prostate cancer cell growth, migration, and tumor progression, highlighting its therapeutic potential in PCa.[21,24,25] Given its regulatory role in tumorigenesis, ferroptosis represents a promising therapeutic way for treating PCa.[26] Studies have proven the effect of statin in treating hepatocellular carcinoma *via* inducing ferroptosis to inhibit MVA pathway,[10,27] but the link between statin-mediated MVA pathway modulation and ferroptosis in PCa has not been established. Collectively, accumulating evidence suggests that aberrant activation of the MVA pathway contributes to PCa progression and that its inhibition may trigger ferroptosis to suppress cancer progression. Therefore, we hypothesized that statins might suppress PCa progression by inhibiting the MVA pathway and inducing ferroptosis. In this study, we treated PCa cells with five statins and identified lovastatin as the most potent inhibitor. Lipid peroxidation assays further revealed that lovastatin significantly elevates ROS levels. These findings might provide novel mechanistic insights into lovastatin's antitumor activity and support the development of personalized therapies for PCa.

Materials and Methods

Cell passage and culture

Cell passage and culture: Human prostate cancer cells PC3 (STCC11203G, Servicebio, Wuhan, China) were cultured in Ham's F-12K (Kaighn's) Medium (21127022, Gibco, Rockville, MD, USA) and DU145 (STCC11203G, Servicebio) were cultured in RPMI 1640 Medium (11875093, Gibco), both media were supplemented with 10% fetal bovine serum (FBS, 164210-500, Procell, Wuhan, China) and 1% penicillin-streptomycin (100 U/mL penicillin, 0.1 mg/mL streptomycin). All cultures were maintained at 37°C in a humidified 5% CO□ incubator.

Drug treatment

PC3 and DU145 cells were treated with five clinical statins - lovastatin, simvastatin, rosuvastatin, atorvastatin, and mevastatin (all purchased from Aladdin Biochemical Technology, Shanghai, China) at concentrations of 1, 3, 10, 30, and 100 μM for 24 h or 48 h. Additional experiments used lovastatin alone or in combination with deferoxamine (DFO, Aladdin Biochemical Technology, Shanghai, China) at 30 μM and mevalonic acid (MVA, MedChemExpress, Monmouth Junction, NJ, USA) at 100 μM.

MTT assay

Cells were uniformly suspended and seeded into 96-well plates at 4,800 cells/well. Following cell attachment and drug exposure for 48 h. MTT (M1020, MTT Cell Proliferation and Cytotoxicity Assay Kit, Solarbio, Beijing, China) solution (0.5 mg/mL final concentration) was added to each well, with subsequent incubation for 4 h. Detection and calculation: Formazan crystals were dissolved in DMSO (MedChemExpress) and absorbance measured at 490 nm using a microplate reader. Half-maximal inhibitory concentration (IC_{50}) values were calculated.

Transwell assay

200 μL of PC3 cells at concentration of 3×10□ in serum-free medium were seeded into the upper chamber, serum-starved for 24 h. 60 μL Matrigel (Corning, Corning, NY, USA) was evenly applied to chamber bottoms and solidified at 37°C for 1 h. Test compounds were prepared in serum-free medium, with medium-only controls. 500 μL complete medium with 10% FBS was added to 24-well plates as chemoattractant. Starved cells were trypsinized, resuspended, and seeded into upper chambers. Cells were treated with various drug concentrations for 24 h. Following 24 h drug treatment, invaded cells were fixed in 4% paraformaldehyde (Chongqing Chuandong Chemical, Chongqing, China),

washed with PBS (Solarbio), and stained with 0.5% crystal violet for 20 min prior to microscopic counting in five random fields. Detailed experimental procedures can be found in a previous report.[28]

Wound healing assay

6-well plates were marked with 0.5 cm spaced grid lines. Cells were seeded to form confluent monolayers. Wounds were created using 200 µL pipette tips perpendicular to marked lines. PBS washed away detached cells and serum residues. Serum-free/low-serum medium containing test compounds was added for 24 h. Migration was documented at 0 h, 24 h and 48 h using inverted microscopy. Wound closure was quantified using ImageJ software. The experiment was conducted according to the procedures described in a previous report.[29]

Fe^{2+} level detection

Kits for this assay is Cell Ferrous Iron (Fe^{2+}) Fluorometric Assay Kit (E-BC-F101, Elabscience, Wuhan, China). Cells were seeded in 12-well plates at an appropriate density according to their growth characteristics. After 24 h of adherent culture, cells were treated according to the experimental protocol for a specified duration. Supernatants from each treatment group were collected. A standard curve was generated using Fe^{2+} standards at concentrations of 0, 5, 10, 15, 20, 30, 40, and 50 µM, following the manufacturer's instructions. 80 µL of each standard solution was mixed with 80 µL of chromogenic reagent per well. 80 µL of each sample supernatant was mixed with 80 µL of chromogenic reagent per well. 80 µL of each sample supernatant was mixed with 80 µL of control reagent per well. After thorough mixing, plates were incubated at 37°C for 10 min, and absorbance was measured at 593 nm using a microplate reader.

Total cholesterol measurement

Kit is Amplex Red Cholesterol and Cholesteryl Ester Assay Kit (S0211S, Beyotime Biotechnology). Cells (50-70% confluency) were treated for 24 h. Use PBS to rinse and remove residual medium. Cells were lysed using BeyoLysis™ Buffer A or isopropanol. Lysates were centrifuged at 600 g for 4 min at 4°C. Cholesterol standards (0-500 µM) were prepared. Samples and standards were reacted with cholesterol detection reagent. Absorbance at 570 nm was measured. Cholesterol concentrations were determined against standard curve.

JC-1 mitochondrial membrane potential assay

Cells were treated for 24 h. PBS washed cells once. JC-1 (E-CK-A301, Mitochondrial Membrane Potential Assay Kit, Elabscience, Wuhan, China) working solution was added for 20 min at 37°C. 1× JC-1 staining buffer was prepared. Cells were trypsinized and centrifuged. Cells were washed twice with JC-1 buffer. Red/green fluorescence was observed under fluorescence microscopes.

Protein extraction and quantification

Cells were washed with cold PBS. Ice-cold lysis buffer was added for 30 min with intermittent shaking. Lysates were centrifuged at 12,000 rpm for 10 min at 4°C. Supernatants were stored at -30°C (short-term) or -80°C (long-term). Reagents A and B (PC0020, Bca Protein Assay Kit, Solarbio) were mixed (50:1). Samples were diluted 20-fold in PBS. BSA standards (0-2000 µg/mL) were prepared. Samples/reactants were incubated at 37°C for 30 min. Absorbance at 562 nm was measured. Protein concentrations were calculated against standard curve.

Western blot analysis

SDS-PAGE gels were cast using appropriate acrylamide concentrations. Samples (20-25 µg protein) were separated at 70 V (30 min) then 120-180 V. Proteins were transferred to PVDF membranes at 330 mA for 1-1.5 h. Membranes were blocked with 5% skim milk for 1 h. Membranes were incubated with primary antibodies overnight at 4°C. HRP-conjugated secondary antibodies were applied for 1 h. ECL substrate was used for chemiluminescent imaging. Band intensities were quantified using ImageJ software. The antibodies used in this experiment are as follows: Goat anti-Rabbit IgG Secondary Antibody (31460, Thermo Fisher, Waltham, MA, USA), Goat anti-Mouse Secondary Antibody (31430, Thermo Fisher), GAPDH (R380626, Zenbio, Shanghai, China), Glutathione Peroxidase 4 (R381958, Zenbio), HMGCR (R24588, Zenbio) HMGCS1 (861746, Zenbio), PTGS2 (Affinity Biosciences, Cincinnati, OH, USA).

Transmission electron microscopy

Cells were treated for 24-48 h. Cells were scraped and centrifuged at 500 g for 5 min. Cell pellets were fixed in 1% osmium tetroxide for 2 h. Gradual acetone dehydration (30-100%). Gradual Epon-812 resin infiltration. Samples were polymerized at 60°C for 24 h. 60-90 nm ultrathin sections were cut. Uranyl acetate and lead citrate staining. JEOL JEM-1400FLASH TEM was used for observation.

Statistical analysis

Data were analyzed using Statistic Package for Social Science (SPSS) 29.0 (IBM, Armonk, NY, USA). Continuous variables are presented as mean ± SD. Between-group comparisons used Student's *t*-test (two groups) or one-way ANOVA with Tukey's post-hoc test (multiple groups). A p-value <0.05 was considered statistically significant.

Results

The effect of statins on the activity of prostate cancer cells

To identify the most potent statin and the prostate cancer cell line with heightened drug sensitivity, we selected five clinically common statins – lovastatin, simvastatin, rosuvastatin, atorvastatin, and mevastatin – and treated two prostate cancer cell lines (PC3 and DU145) with six graded concentrations of each drug. Cell viability was assessed via MTT assays to evaluate inhibitory effects. As illustrated in Figure 1 A,B, the PC3 cell line exhibited significantly lower survival rates under statin treatment compared to DU145. Consequently, PC3 was selected as the primary model for subsequent investigations.

After identifying the candidate drug and cell line, this study employed MTT assays to evaluate the effects of lovastatin (LV) at varying concentrations on PC3 cell proliferation after 24 h and 48 h of treatment (Figure 1 A,B). As demonstrated, compared to the control group, PC3 cell viability progressively decreased with increasing LV concentration and treatment duration, indicating that LV inhibits PC3 cell proliferation in a concentration-and time-dependent manner. To further investigate the specific effects of LV on the migratory and invasive capacities of prostate cancer cells, we conducted Transwell assays to evaluate these characteristics in PC3 cells following drug treatment. As shown in Figure 1C, compared to the control group, lovastatin-treated groups (5 µM and 10 µM) exhibited significantly reduced numbers of PC3 cells migrat-

ing through and invading across the Transwell chamber membrane, indicating that LV markedly inhibited the migratory and invasive abilities of PC3 cells (Figure 1D). Furthermore, to validate these findings, we performed wound healing assays to assess the migration rate of PC3 cells under LV treatment. As demonstrated in Figure 1E, after 24 h and 48 h of treatment with 5 μM LV, the wound closure rates were significantly lower than those in the control group. These results, consistent with the Transwell assay data,

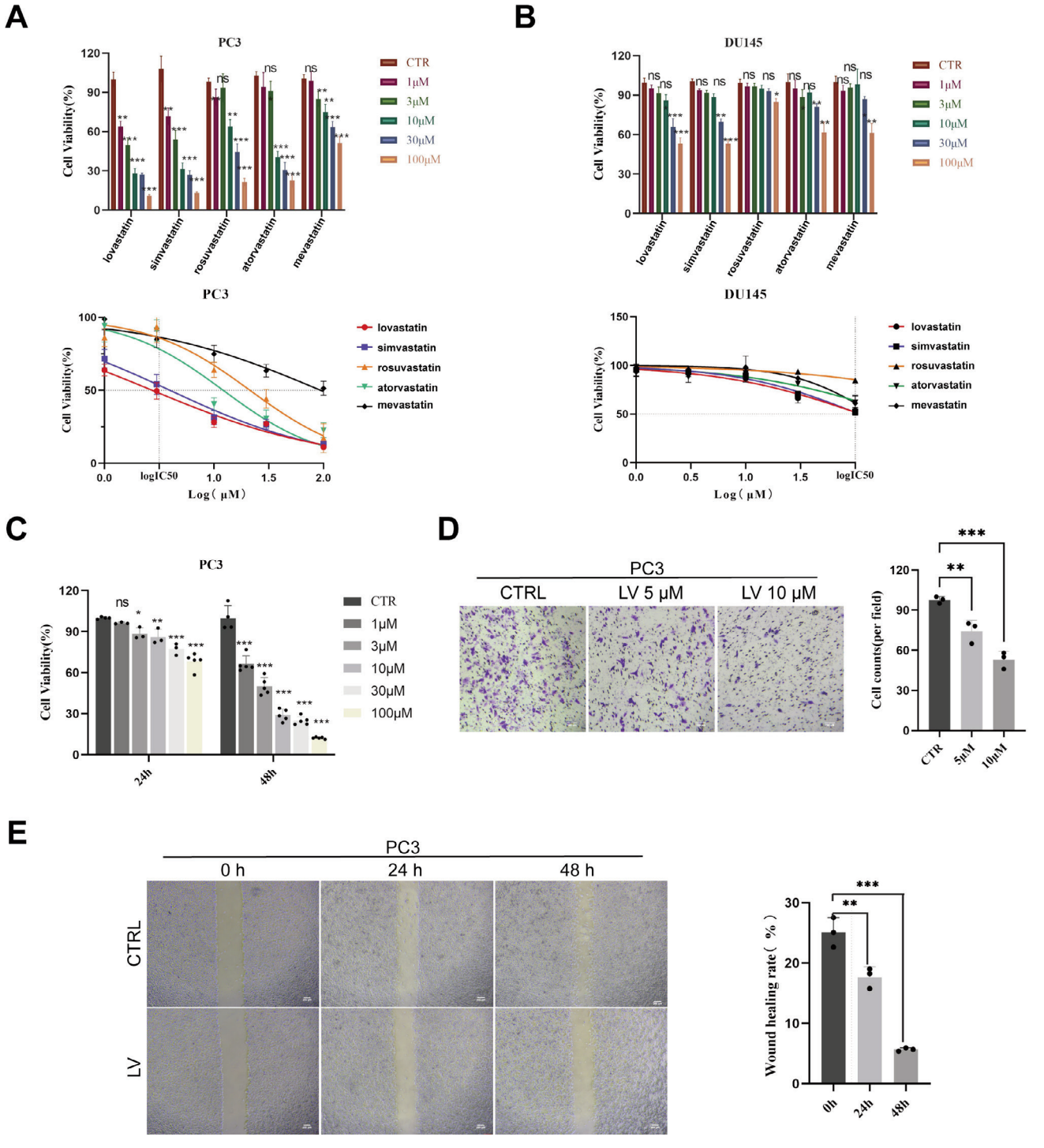

Figure 1. The effect of statins on the activity of prostate cancer cells. **A**) Bar graph and survival rate curve showing the effects of statins on PC3 cells. **B**) Bar graph and survival rate curve showing the effects of statins on DU145 cells. **C**) The survival rate of PC3 cells after treatment with lovastatin; ns, no statistically significant difference. **D**) Wound healing rate of PC3 cells after treatment with statins; scale bar: 100 μm. **E**) Microscopic images from the wound healing assay; statistical graph of wound healing rates were shown on the right. scale bar: 100 μm; n=5; *p>0.05, **p<0.01; ***p<0.001.

further confirm the inhibitory effect of LV on PC3 cell motility. Collectively, these findings demonstrate that LV not only suppresses PC3 cell proliferation but also effectively reduces their migratory and invasive capacities.

LV induces ferroptosis in prostate cancer cells

Iron deposition represents a critical pathological feature of ferroptosis. DFO, a highly effective iron chelator, has been extensively studied in various degenerative disease models and demonstrated to effectively prevent ferroptosis. To investigate the potential mechanisms underlying LV-induced PC3 cell death, we examined the effects of LV in combination with DFO. Subsequent experiments were conducted using 5 μM LV and 30 μM DFO. As shown in Figure 2A, compared to the control group, LV treatment significantly reduced cell proliferation activity. Notably, this LV-induced decrease in PC3 cell viability was markedly attenuated by DFO co-treatment. These results suggest that LV may exert its effects, at least in part, through induction of ferroptosis in PC3 cells.

To further investigate whether LV induces PC3 cell death through ferroptosis, we first examined intracellular Fe^{2+} levels. As shown in Figure 2B, LV treatment significantly increased Fe^{2+} content in PC3 cells. However, co-treatment with the iron chelator DFO markedly reduced Fe^{2+} levels. These data suggest that LV may trigger ferroptosis-related pathways by enhancing intracellular iron accumulation, ultimately leading to decreased PC3 cell viability. These results clearly demonstrate that LV promotes intracellular Fe^{2+} accumulation, potentially through activation of ferroptosis signaling pathways, resulting in significantly reduced PC3 cell survival. Furthermore, the inhibitory effect of DFO further confirms the pivotal regulatory role of iron in this process.

Excessive intracellular ROS accumulation is a hallmark characteristic of ferroptosis.[30,31] To further validate the ferroptosis-inducing effect of LV in PC3 cells, we specifically analyzed alterations in intracellular ROS levels following drug treatment. As illustrated in Figure 2C, quantitative analysis revealed that LV treatment significantly elevated ROS levels in PC3 cells. Notably, co-treatment with the iron chelator DFO substantially reduced ROS levels, providing additional evidence that LV may induce prostate cancer cell death through ferroptosis activation.

Combined treatment with DFO improved intracellular damage caused by lovastatin

Ferroptosis is a distinct form of programmed cell death,[32] characterized by iron-dependent phospholipid peroxidation, ultimately leading to plasma membrane damage and cell death. In this process, phospholipid peroxidation serves as a key driver, though cells pos-

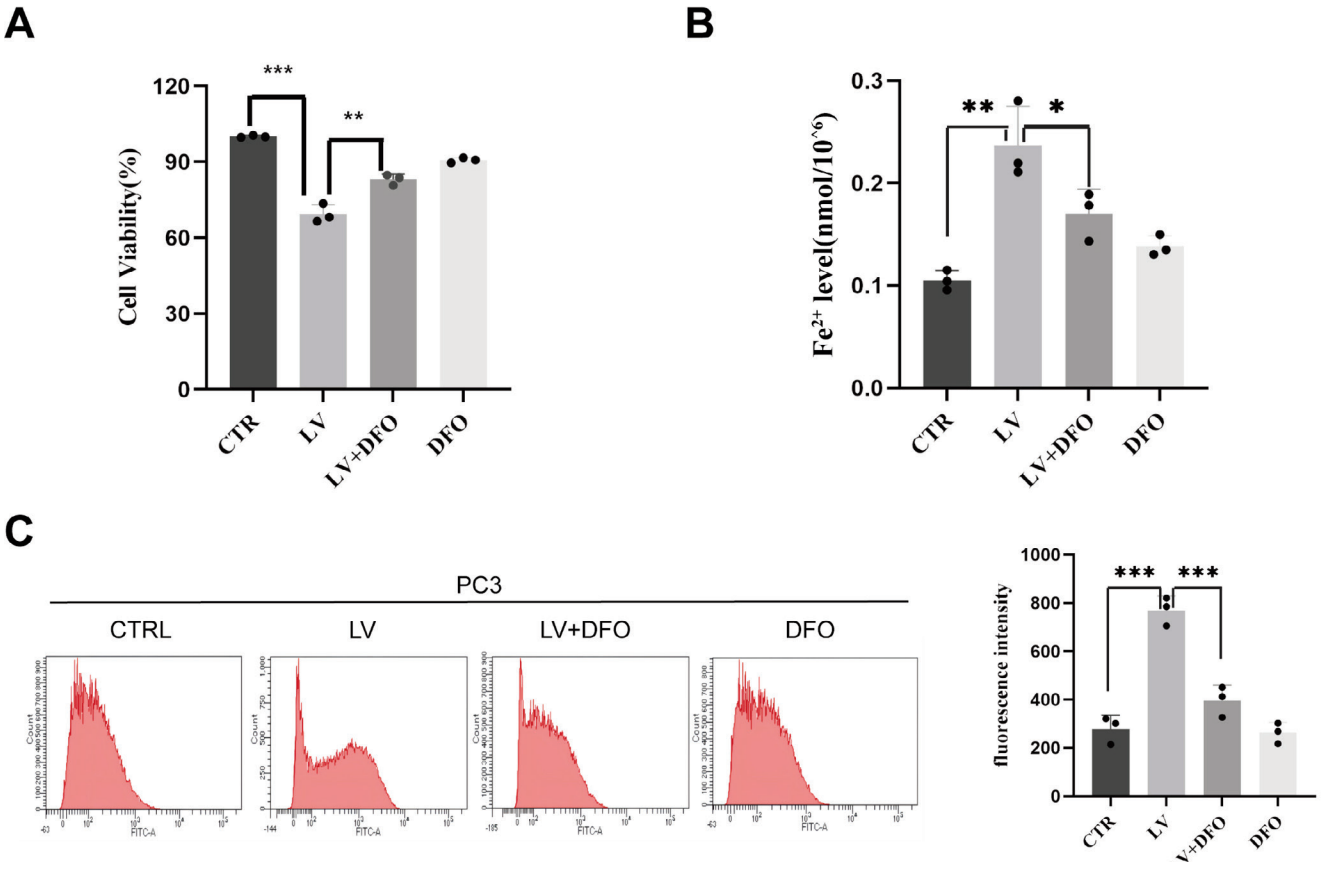

Figure 2. LV induces ferroptosis in prostate cancer cells. **A**) Survival rate of PC3 cells after treatment with lovastatin and/or DFO. **B**) Intracellular Fe^{2+} levels after co-treatment with ferroptosis inhibitors. **C**) Quantification of fluorescence intensity by flow cytometer; quantitative analysis of fluorescence intensity was on the right. ns, no statistically significant difference; n=3; *p>0.05, **p<0.01; ***p<0.001.

sess a surveillance mechanism to prevent unnecessary ferroptosis.[20] Notably, glutathione peroxidase 4 (GPX4) is a central regulator of ferroptosis. GPX4, a monomeric glutathione peroxidase, plays a critical protective role by reducing phospholipid hydroperoxides to their corresponding alcohols, thereby inhibiting membrane lipid peroxidation. Studies have demonstrated that GPX4 depletion significantly induces ferroptosis.[32,33] The activity of GPX4 depends on its essential reductant, glutathione (GSH). Through GPX4, GSH mitigates reactive nitrogen species (RNS) and reactive oxygen species (ROS), maintaining intracellular redox homeostasis. Thus, GPX4 and its upstream metabolic pathways constitute one of the major inhibitory mechanisms against ferroptosis.[32] Additionally, prostaglandin-

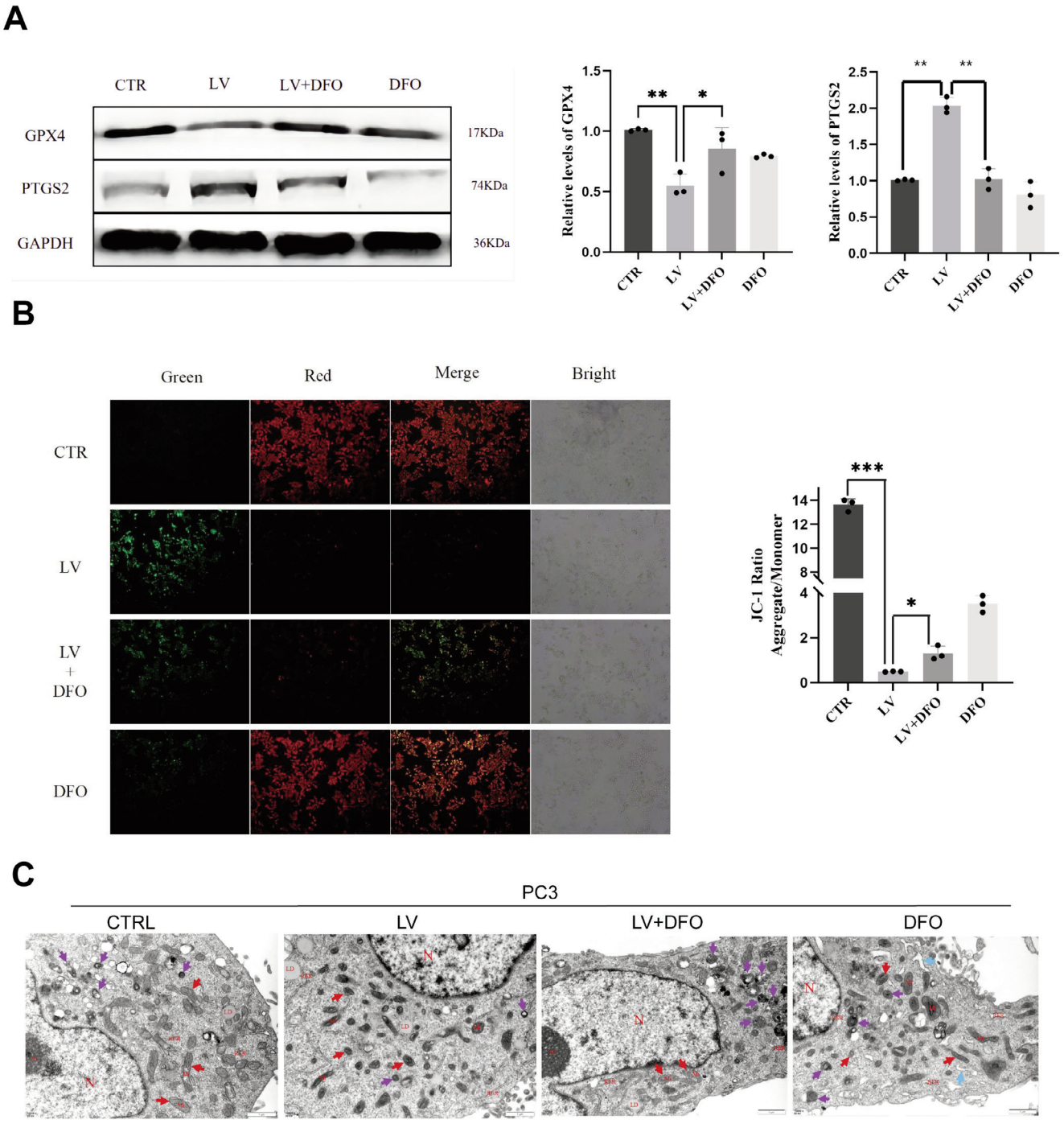

Figure 3. Combined treatment with DFO improved intracellular damage caused by lovastatin. **A**) Western blot showing changes in GPX4 and PTGS2 proteins; statistical analysis of GPX4 and PTGS2 protein changes was on the right. **B**) Image of fluorescence intensity; quantitative analysis of the ratio of red fluorescence intensity to green fluorescence intensity was on the right. **C**) Morphological changes in cells after co-treatment with ferroptosis inhibitors; N, nucleus; No, nucleolus; Mi, mitochondria; RER, rough endoplasmic reticulum; LD, lipid droplet; scale bar: 1 μm; ns, no statistically significant difference; n=3; *p>0.05, **p<0.01; ***p<0.001.

endoperoxide synthase 2 (PTGS2), a key enzyme in prostaglandin biosynthesis, has been identified as a biomarker of ferroptosis.[20] To investigate whether LV exerts its effects in PC3 cells by modulating ferroptosis-related proteins, we analyzed GPX4 protein expression levels via Western blotting. Experimental results (Figure 3A) revealed that compared to the control group, lovastatin treatment significantly reduced GPX4 expression, suggesting that lovastatin may promote ferroptosis by downregulating GPX4. Furthermore, when the iron chelator DFO was co-administered, GPX4 expression was restored. In contrast, PTGS2 protein levels were markedly elevated after lovastatin treatment, whereas DFO co-treatment significantly attenuated this increase, implying that PTGS2 upregulation may be associated with enhanced membrane lipid peroxidation. These findings further substantiate that lovastatin likely induces prostate cancer cell death by triggering ferroptosis. The mitochondrial membrane potential (MMP), generated by the proton gradient across the inner mitochondrial membrane (with the matrix side being negatively charged), serves as a critical indicator of mitochondrial function and homeostasis. This electrochemical gradient not only plays a pivotal role in cellular energy metabolism but is also intimately associated with apoptotic signaling pathways.[34,35] A reduction in MMP is generally regarded as a hallmark of mitochondrial damage and represents one of the early events in the initiation of mitochondria-mediated apoptosis. JC-1, a sensitive fluorescent probe, is widely employed as a MMP indicator due to its potential-dependent accumulation in mitochondria. This dye exhibits distinct fluorescence properties depending on MMP status: at high MMP, JC-1 forms aggregates in the mitochondrial matrix that emit red fluorescence (~590 nm), while at low MMP, it remains in monomeric form, producing green fluorescence (~530 nm).[36] The ratio of red-to-green fluorescence intensity provides a quantitative measure of MMP changes. To investigate the impact of LV on mitochondrial function in PC3 cells, we performed JC-1 staining coupled with immunofluorescence analysis to monitor dynamic MMP changes following drug treatment. As shown in (Figure 3B), LV treatment significantly reduced MMP in PC3 cells, as evidenced by decreased red fluorescence intensity and concomitant increase in green fluorescence, indicating mitochondrial impairment. To examine whether this effect was associated with ferroptosis, we employed the iron chelator DFO as an intervention. Notably, DFO co-treatment substantially attenuated the LV-induced MMP dissipation, with the red/green fluorescence ratio increased. These data further support the hypothesis that LV induces PC3 cell damage through ferroptosis-mediated mitochondrial dysfunction. To more intuitively observe the morphological changes in PC3 cells following LV treatment, we conducted detailed ultrastructural analysis using transmission electron microscopy (TEM). Normal control cells exhibited elongated or oval mitochondria with intact double membranes and well-organized internal structures,[37] whereas ferroptosis-induced mitochondria displayed characteristic features including significant volume shrinkage, increased membrane density, and reduction/loss of cristae.[38] Notably, while these mitochondrial changes were prominent, nuclear morphology and chromatin organization remained largely unaffected, with rough endoplasmic reticulum maintaining parallel arrangements and autolysosomes appearing as single-membrane vesicles containing degraded cytoplasmic components. Our TEM results (Figure 3C) revealed that LV treatment induced marked mitochondrial condensation with reduced volume, widened intercristal spaces, increased matrix electron density, and substantial cristae reduction - all hallmarks of ferroptosis. Importantly, co-treatment with DFO significantly attenuated these mitochondrial abnormalities, suggesting the protective role of DFO against LV-induced damage. These findings not only substantiate LV's ability to induce ferroptosis in PC3 cells but also demonstrate that ferroptosis inhibition can mitigate drug-induced mitochondrial injury, providing mechanistic insights into LV's antitumor effects while highlighting potential therapeutic applications of ferroptosis modulation in cytoprotection and side-effect management.

LV promotes ferroptosis in prostate cancer cells by inhibiting the MVA pathway

To investigate whether LV-induced cytotoxicity in PC3 cells involves the MVA pathway, we performed rescue experiments with MVA co-treatment (5 μM LV + 100 μM MVA). Notably, MVA supplementation significantly reversed LV-mediated cell death, suggesting that MVA pathway inhibition critically contributes to the cytotoxic effects of LV, potentially via ferroptosis induction (Figure 4A). This finding implies that MVA-derived metabolites may regulate ferroptosis sensitivity through mitochondrial function modulation, oxidative stress responses, or membrane stability alterations via phospholipid peroxidation. Given the MVA pathway's pleiotropic roles in cellular metabolism, these results not only elucidate a novel mechanism underlying the anti-cancer activity of LV but also support therapeutic targeting of this metabolic pathway. The MVA pathway is a highly conserved metabolic route in eukaryotes responsible for generating isoprenoid units that serve as fundamental building blocks for various biomolecules, including cholesterol, steroid hormones, vitamin K, and coenzyme Q.[39] As one of the terminal products of the MVA pathway, cholesterol plays crucial roles in maintaining membrane integrity, cellular signaling, and other essential biological processes.[39] This pathway is regulated by several key enzymes, notably 3-hydroxy-3-methylglutaryl-CoA reductase (HMGCR), which represents the primary pharmacological target of statins such as lovastatin. To elucidate the involvement of the MVA pathway in LV -induced ferroptosis in PC3 cells, we specifically examined intracellular cholesterol levels. As demonstrated in (Figure 4B), LV treatment alone significantly reduced cellular cholesterol content to 0.16 mmol/L. However, concomitant administration of MVA substantially restored cholesterol levels to 0.317 mmol/L. These findings suggest that cholesterol, as a critical metabolic product of the MVA pathway, may play a pivotal role in mitigating LV-triggered ferroptosis. This observation not only reinforces the potential regulatory function of the MVA pathway in prostate cancer cell ferroptosis but also provides novel experimental evidence for understanding the mechanistic basis of LV's antitumor effects. To further investigate the molecular mechanisms underlying effects of in PC3 cells, we performed Western blot analysis to examine expression changes of key proteins in the MVA pathway, including 3-hydroxy-3-methylglutaryl-CoA reductase (HMGCR), 3-hydroxy-3-methylglutaryl-CoA synthase 1 (HMGCS1), and farnesyl pyrophosphate synthase 1 (FDFT1). As shown in (Figure 4C), LV treatment significantly reduced protein expression levels of these enzymes compared to the control groups, demonstrating that LV exerts significant metabolic effects through inhibition of the MVA pathway.

In order to investigate whether LV affects PC3 cell viability through ferroptosis induction, we next measured intracellular Fe^{2+} concentrations following drug treatment. As demonstrated in Figure 4, LV treatment significantly increased Fe^{2+} levels in PC3 cells, indicating LV is able to promote intracellular iron accumulation. Notably, combined treatment with LV and MVA pathway components significantly reduced Fe^{2+} concentrations compared to LV monotherapy (Figure 4D). These findings suggest that MVA pathway inhibition may facilitate ferroptosis in PC3 cells by modulating intracellular iron metabolism.

To further elucidate the effects of LV on PC3 cells following MVA co-treatment, we examined alterations in intracellular ROS levels. As illustrated in Figure 4E, LV treatment significantly ele-

vated ROS levels in PC3 cells compared to the control group, indicating marked enhancement of oxidative stress - a hallmark characteristic of ferroptosis. Notably, concomitant administration of MVA substantially attenuated this ROS accumulation. These findings provide additional evidence supporting the regulatory role of the MVA pathway in lovastatin-induced ferroptosis.

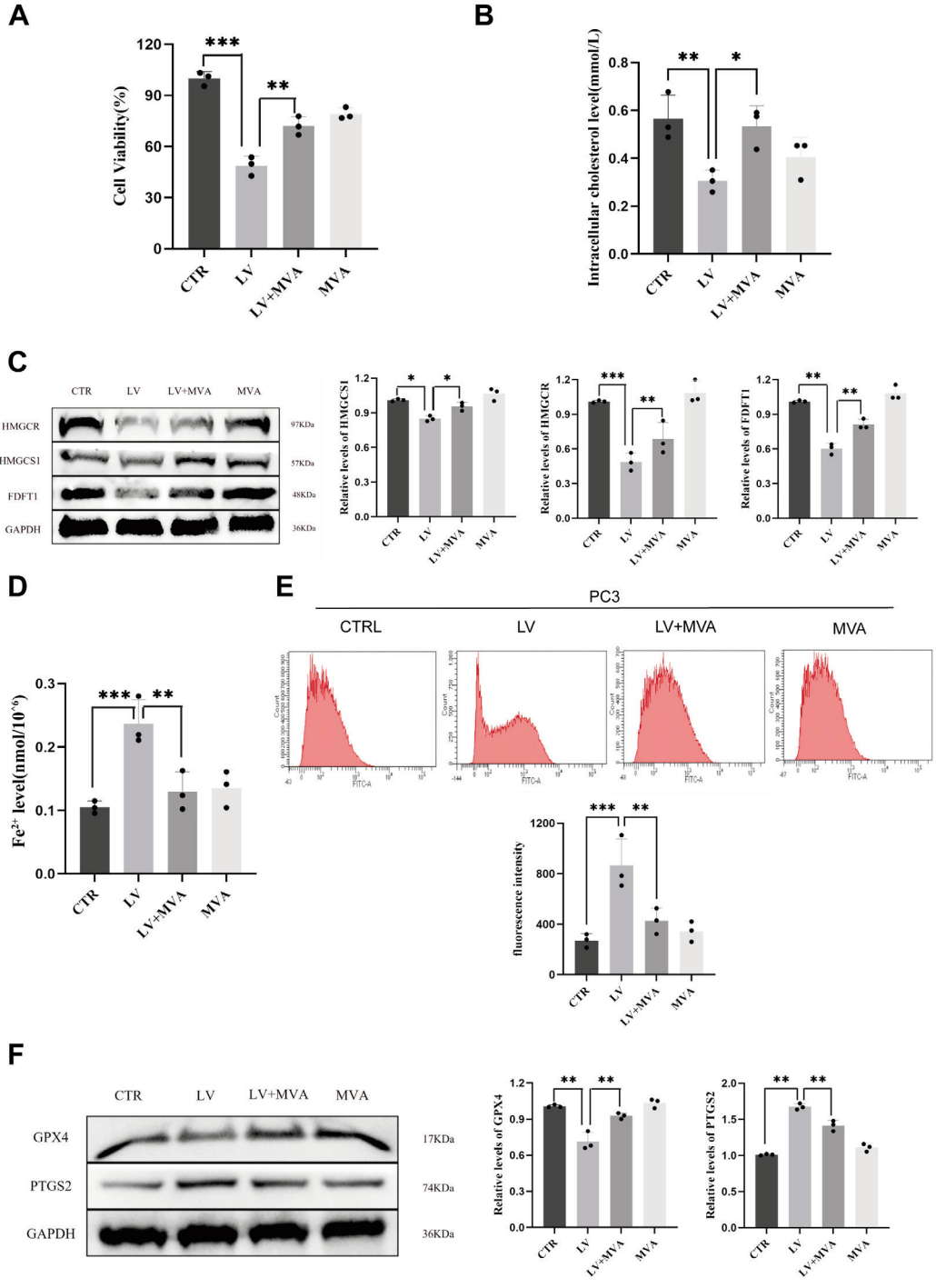

Figure 4. LV promotes ferroptosis in prostate cancer cells by inhibiting the MVA pathway. **A**) Survival rate of PC3 cells after treatment with lovastatin and/or MVA. **B)** Intracellular cholesterol level after treatment with lovastatin and/or MVA. **C**) Western blot of intracellular HMGCR, HMGCS1, and FDFT1 protein levels after co-treatment with MVA; quantitative analysis of HMGCR, HMGCS1, and FDFT1protein expression levels was on the right. **D**) Intracellular Fe2+ levels after co-treatment with MVA. **E**) Intracellular ROS levels after co-treatment with ferroptosis inhibitors; quantitative analysis of fluorescence intensity was below. **F**) Intracellular GPX4 and PTGS2 protein levels after co-treatment with MVA; quantitative analysis of GPX4 and PTGS2 protein expression levels. ns, no statistically significant difference; n=3; **p*>0.05, ***p*<0.01; ****p*<0.001.

We next investigated the expression changes of ferroptosis-related proteins GPX4 and PTGS2 in PC3 cells by Western blot analysis. The results demonstrated that LV treatment significantly decreased GPX4 protein levels, while co-treatment with MVA restored its expression (Figure 4F). Conversely, PTGS2 protein levels showed an opposite trend, increased after LV treatment and decreased with MVA treatment. These findings further support the conclusion that LV induces PC3 cell death through ferroptosis activation. As a crucial antioxidant enzyme, GPX4 plays a pivotal role in ferroptosis by suppressing lipid peroxide accumulation. The observed downregulation of GPX4 following LV treatment likely compromises cellular antioxidant capacity, thereby accelerating lipid peroxidation and membrane damage. Moreover, PTGS2 upregulation is recognized as a key biomarker of lipid peroxidation and is closely associated with ferroptosis. In this study, MVA supplementation effectively restored GPX4 expression and attenuated PTGS2 overexpression, suggesting that the MVA pathway may mitigate lovastatin-induced ferroptosis by modulating cellular antioxidant systems and lipid metabolism.

Discussion

PCa is one of the most common malignant tumors in men, characterized by a slow but highly invasive disease progression, making it a clinical challenge due to its invasive nature and the emergence of drug resistance.[1-3] Although early screening technologies and treatment methods have advanced in recent years, leading to some improvement in patient survival rates, conventional treatments such as surgery, radiotherapy, and chemotherapy often yield unsatisfactory outcomes in advanced cases due to the disease's typically slow and complex progression.[5] Additionally, drug resistance and disease recurrence have become major challenges in current treatment strategies. Therefore, further research into the pathogenesis of prostate cancer and understanding the biological mechanisms of PCa is essential for identifying novel therapeutic targets to improve prognosis. Studying prostate cancer helps to better understand its biological characteristics and pathogenic mechanisms, thereby enabling the development of more effective prevention and treatment measures. For instance, improving the sensitivity and accuracy of early screening could significantly enhance early diagnosis rates, while research on personalized treatment strategies may reduce side effects associated with conventional therapies. There is an urgent need to explore new therapeutic targets and anticancer drugs for prostate cancer to provide more options for improving patients' quality of life.

While primarily prescribed as lipid-lowering agents, statins have recently demonstrated therapeutic potential in various malignancies through anti-proliferative and pro-apoptotic mechanisms.[8,9,40] Through in-depth investigation of their mechanisms of action, this study explores the potential of LV in prostate cancer treatment, providing theoretical foundations and experimental data for developing novel anticancer drugs. By analyzing the anticancer potential of statins, especially their role in regulating prostate cancer metabolism and cell death mechanisms, this study offers new perspectives and potential therapeutic targets for anticancer treatment.

Statins exert multifaceted antitumor effects by modulating cell cycle regulation, apoptosis, and angiogenesis.[40] MVA metabolic pathway has been identified as an important target for tumor cell growth. This pathway participates in the synthesis of cholesterol and isoprenoid molecules, which are crucial for rapid tumor cell proliferation.[13,14] By inhibiting HMGCR, a key enzyme in the MVA pathway, statins can effectively suppress tumor cell growth and induce tumor cell death.[40,41] As a representative statin, LV has well-established safety profiles and favorable pharmacokinetic properties, making it widely studied for its potential in cancer treatment. This study further validates the mechanism by which LV inhibits prostate cancer cell growth through MVA pathway-induced ferroptosis, providing new evidence for understanding the antitumor mechanisms of statins.

In this study, experimental results showed that among five statins tested, LV exhibited the most significant inhibitory effect on prostate cancer cells. Our multi-modal analysis, including Western blot and electron microscopy, confirms that LV-induced ferroptosis is characterized by ROS/Fe^{2++} elevation and specific mitochondrial morphological changes, which are effectively reversed by DFO. Unlike traditional apoptosis, ferroptosis, an iron-dependent form of cell death, has emerged as a vital regulatory mechanism and a promising therapeutic target across various malignancies like cancer.[19] This study is the first to systematically demonstrate that LV induces ferroptosis through regulation of the MVA pathway. Western blot analysis revealed that LV treatment significantly upregulated the expression of ferroptosis-related proteins GPX4 and PTGS2, and these changes were reversed by DFO co-treatment. Furthermore, transmission electron microscopy observations showed characteristic mitochondrial morphological changes in lovastatin-treated prostate cancer cells, which were alleviated after DFO intervention. These findings not only further clarify the important role of ferroptosis in prostate cancer treatment but also provide experimental evidence for its potential as a therapeutic target.

MTT assays demonstrated that LV significantly reduced cell viability in PC3 prostate cancer cells, and this antiproliferative effect was markedly attenuated when combined with MVA. The observation suggests that MVA supplementation reverses LV-induced cytotoxicity, apoptosis, and cholesterol depletion underscores the central role of the MVA pathway in maintaining PCa cell survival. By restoring cholesterol levels essential for membrane synthesis and energy metabolism, MVA supplementation effectively antagonizes lovastatin-induced metabolic stress. Key proteins in the MVA pathway (such as HMGCS1, HMGCR, and FDFT1) play central roles in MVA metabolism. Western blot analysis showed that expression levels of these proteins were significantly decreased in the LV-treated group, while MVA supplementation reversed these changes. This indicates that LV suppresses metabolic activity by downregulating key enzymes in the MVA pathway, while MVA supplementation partially restores normal cellular metabolism. Additionally, experimental results showed that MVA co-treatment significantly mitigates LV-induced elevation of ROS and Fe^{2+}, suggesting that the MVA pathway serves as a critical regulator of cellular redox balance and iron metabolism. Furthermore, the regulatory role of MVA pathway is further demonstrated by the reversal of LV-induced GPX4 downregulation and PTGS2 upregulation upon MVA supplementation, confirming its necessity in ferroptosis inhibition. This further demonstrates the important regulatory role of the MVA pathway in lovastatin-induced ferroptosis.

These findings not only further support the mechanism by which LV induces ferroptosis through MVA pathway inhibition but also emphasize the importance of the MVA pathway in maintaining the balance between cell survival and death. MVA supplementation significantly attenuates lovastatin's anticancer effects by restoring metabolic homeostasis, regulating key enzyme expression, and reducing oxidative stress levels. This suggests that tumor cells may activate metabolic compensation mechanisms to counteract lovastatin's inhibitory effects. These findings suggest that the efficacy of statin therapy in clinical settings may be context-dependent, contingent upon the metabolic state of the tumor. Moreover, this

mechanistic insight opens new possibilities for developing combination therapies, such as enhancing statins' anticancer efficacy by inhibiting metabolic compensation mechanisms.

This study is the first to reveal that LV inhibits prostate cancer cell growth by suppressing key enzymes in the MVA pathway and inducing ferroptosis. By filling the knowledge gap regarding the MVA-ferroptosis axis in PCa, our study identifies metabolic compensation, specifically MVA uptake, as a key resistance mechanism. Targeting these pathways offers a promising strategy for developing synergistic combination therapies with statins.

However, this study has several limitations that need to be addressed: First, while statins can induce cancer cell death through multiple pathways, this study only examined lovastatin's antiproliferative effects through ferroptosis induction in prostate cells. Other potential cell death pathways such as apoptosis, necrosis, and pyroptosis should be investigated to comprehensively understand its mechanisms of action. Second, when examining ferroptosis-related indicators, lipid ROS could be included as a more direct measure of ferroptosis. Finally, as this study was conducted entirely in vitro, future work should incorporate cell- or patient-derived xenograft mouse models to better validate lovastatin's antitumor efficacy. Our findings demonstrate that lovastatin exerts potent antitumor effects in PCa by disrupting the MVA pathway and triggering ferroptosis. Mechanistically, lovastatin treatment elevated ROS and Fe^{2+} levels, impaired mitochondrial function, downregulated GPX4, and upregulated PTGS2, all of which were reversed by the ferroptosis inhibitor DFO. Notably, MVA pathway supplementation rescued cell viability and restored GPX4 expression, confirming the critical role of MVA signaling in lovastatin-induced ferroptosis. These results not only elucidate the molecular basis of statin-mediated anticancer activity but also propose targeting the MVA-ferroptosis axis as a novel therapeutic strategy for PCa. Further preclinical and clinical studies are warranted to translate these findings into potential therapeutic applications.

In conclusion, our study identifies lovastatin as a potent antitumor agent in PCa, acting through the dual mechanisms of MVA pathway disruption and ferroptosis induction. Mechanistically, we demonstrate that lovastatin-induced metabolic stress leads to lethal iron-dependent lipid peroxidation and mitochondrial dysfunction, a process strictly dependent on the exhaustion of MVA-derived metabolites. By confirming that MVA supplementation completely abrogates these effects, this research establishes the MVA pathway as a pivotal metabolic switch governing ferroptosis sensitivity in prostate cancer cells. These findings provide a strong mechanistic rationale for repurposing lovastatin to bypass traditional drug resistance in PCa by targeting the MVA-ferroptosis axis, offering a precision metabolic approach to cancer therapy. Future research should focus on optimizing combination regimens that synergistically inhibit MVA flux to maximize the clinical efficacy of pro-ferroptotic interventions in advanced PCa patients.

References

1. Sung H, Ferlay J, Siegel RL, Laversanne M, Soerjomataram I, Jemal A, et al. Global Cancer Statistics 2020: GLOBOCAN estimates of incidence and mortality worldwide for 36 cancers in 185 countries. CA Cancer J Clin 2021;71:209-49.
2. Chen W, Xu L, Deng H, Zhu Z, Yang D. Role of USP10/METTL3/CXCR4 axis in immunotherapy of castration-resistant prostate cancer. Iran J Allergy Asthma Immunol 2025;24:334-46.
3. Foreman KJ, Marquez N, Dolgert A, Fukutaki K, Fullman N, McGaughey M, et al. Forecasting life expectancy, years of life lost, and all-cause and cause-specific mortality for 250 causes of death: reference and alternative scenarios for 2016-40 for 195 countries and territories. Lancet 2018;392:2052-90.
4. Sandhu S, Moore CM, Chiong E, Beltran H, Bristow RG, Williams SG. Prostate cancer. Lancet 2021;398:1075-90.
5. Teo MY, Rathkopf DE, Kantoff P. Treatment of advanced prostate cancer. Annu Rev Med 2019;70:479-99.
6. Cheng Q, Butler W, Zhou Y, Zhang H, Tang L, Perkinson K, et al. Pre-existing castration-resistant prostate cancer-like cells in primary prostate cancer promote resistance to hormonal therapy. Eur Urol 2022;81:446-55.
7. Zahedipour F, Butler AE, Eid AH, Sahebkar A. Pleiotropic properties of statins via angiogenesis modulation in cardiovascular disease. Drug Discov Today 2022;27:103325.
8. Borgquist S, Bjarnadottir O, Kimbung S, Ahern TP. Statins: a role in breast cancer therapy? J Intern Med 2018;284:346-57.
9. Vettenranta A, Murtola TJ, Raitanen J, Raittinen P, Talala K, Taari K, et al. Outcomes of screening for prostate cancer among men who use statins. JAMA Oncol 2022;8:61-8.
10. Yao X, Xie R, Cao Y, Tang J, Men Y, Peng H, et al. Simvastatin induced ferroptosis for triple-negative breast cancer therapy. J Nanobiotechnology 2021;19:311.
11. Li Y, Chen S, Zhu J, Zheng C, Wu M, Xue L, et al. Lovastatin enhances chemosensitivity of paclitaxel-resistant prostate cancer cells through inhibition of CYP2C8. Biochem Biophys Res Commun 2022;589:85-91.
12. Guo C, Wan R, He Y, Lin SH, Cao J, Qiu Y, et al. Therapeutic targeting of the mevalonate-geranylgeranyl diphosphate pathway with statins overcomes chemotherapy resistance in small cell lung cancer. Nat Cancer 2022;3:614-28.
13. Gobel A, Riffel RM, Hofbauer LC, Rachner TD. The mevalonate pathway in breast cancer biology. Cancer Lett 2022;542:215761.
14. Guerra B, Recio C, Aranda-Tavio H, Guerra-Rodriguez M, Garcia-Castellano JM, Fernandez-Perez L. The mevalonate pathway, a metabolic target in cancer therapy. Front Oncol 2021;11:626971.
15. Bruzzese F, Pucci B, Milone MR, Ciardiello C, Franco R, Chianese MI, et al. Panobinostat synergizes with zoledronic acid in prostate cancer and multiple myeloma models by increasing ROS and modulating mevalonate and p38-MAPK pathways. Cell Death Dis 2013;4:e878.
16. Lin G, Huang T, Zhang X, Wang G. Deubiquitinase USP35 stabilizes BRPF1 to activate mevalonate (MVA) metabolism during prostate tumorigenesis. Cell Death Discov 2022;8:453.
17. Bathaie SZ, Ashrafi M, Azizian M, Tamanoi F. Mevalonate pathway and human cancers. Curr Mol Pharmacol 2017;10:77-85.
18. Gales L, Forsea L, Mitrea D, Stefanica I, Stanculescu I, Mitrica R, et al. Antidiabetics, anthelmintics, statins, and beta-blockers as co-adjuvant drugs in cancer therapy. Medicina (Kaunas) 2022;58.
19. Jiang X, Stockwell BR, Conrad M. Ferroptosis: mechanisms, biology and role in disease. Nat Rev Mol Cell Biol 2021;22:266-82.
20. Tang D, Chen X, Kang R, Kroemer G. Ferroptosis: molecular mechanisms and health implications. Cell Res 2021;31:107-25.
21. Ghoochani A, Hsu EC, Aslan M, Rice MA, Nguyen HM, Brooks JD, et al. Ferroptosis inducers are a novel therapeutic approach for advanced prostate cancer. Cancer Res 2021;81:1583-94.
22. Zhou X, Zou L, Liao H, Luo J, Yang T, Wu J, et al. Abrogation

of HnRNP L enhances anti-PD-1 therapy efficacy via diminishing PD-L1 and promoting CD8(+) T cell-mediated ferroptosis in castration-resistant prostate cancer. Acta Pharm Sin B 2022;12:692-707.
23. Zheng D, Liu J, Piao H, Zhu Z, Wei R, Liu K. ROS-triggered endothelial cell death mechanisms: Focus on pyroptosis, parthanatos, and ferroptosis. Front Immunol 2022;13:1039241.
24. Zaffaroni N, Beretta GL. Ferroptosis inducers for prostate cancer therapy. Curr Med Chem 2022;29:4185-201.
25. Zhou X, Zou L, Chen W, Yang T, Luo J, Wu K, et al. Flubendazole, FDA-approved anthelmintic, elicits valid antitumor effects by targeting P53 and promoting ferroptosis in castration-resistant prostate cancer. Pharmacol Res 2021; 164:105305.
26. Wang S, Wei W, Ma N, Qu Y, Liu Q. Molecular mechanisms of ferroptosis and its role in prostate cancer therapy. Crit Rev Oncol Hematol 2022;176:103732.
27. Kitsugi K, Noritake H, Matsumoto M, Hanaoka T, Umemura M, Yamashita M, et al. Simvastatin inhibits hepatic stellate cells activation by regulating the ferroptosis signaling pathway. Biochim Biophys Acta Mol Basis Dis 2023;1869:166750.
28. Li Y, Wang Y, Gao J, Xu W, Wang Y, Zhang F. SP1-Induced LncRNA ZFAS1 Contributes to cell proliferation and migration in gastric cancer through AKT/mTOR signaling. Iran J Biotechnol 2025;23:e4071.
29. Wang L, Cao J, Chen H, Xue N, Yu H, Zhao S, et al. Cardiac troponin I Promotes the development of NSCLC cells through the expression of Notch and Kras proteins. Iran J Biotechnol 2025;23:e3976.
30. Park E, Chung SW. ROS-mediated autophagy increases intracellular iron levels and ferroptosis by ferritin and transferrin receptor regulation. Cell Death Dis 2019;10:822.
31. Stockwell BR. Ferroptosis turns 10: Emerging mechanisms, physiological functions, and therapeutic applications. Cell 2022;185:2401-21.
32. Liang D, Feng Y, Zandkarimi F, Wang H, Zhang Z, Kim J, et al. Ferroptosis surveillance independent of GPX4 and differentially regulated by sex hormones. Cell 2023;186:2748-64 e22.
33. Liu Y, Wan Y, Jiang Y, Zhang L, Cheng W. GPX4: The hub of lipid oxidation, ferroptosis, disease and treatment. Biochim Biophys Acta Rev Cancer 2023;1878:188890.
34. Jiao H, Jiang D, Hu X, Du W, Ji L, Yang Y, et al. Mitocytosis, a migrasome-mediated mitochondrial quality-control process. Cell 2021;184:2896-910 e13.
35. Zorov DB, Juhaszova M, Sollott SJ. Mitochondrial reactive oxygen species (ROS) and ROS-induced ROS release. Physiol Rev 2014;94:909-50.
36. Perelman A, Wachtel C, Cohen M, Haupt S, Shapiro H, Tzur A. JC-1: alternative excitation wavelengths facilitate mitochondrial membrane potential cytometry. Cell Death Dis 2012;3:e430.
37. Lam SS, Martell JD, Kamer KJ, Deerinck TJ, Ellisman MH, Mootha VK, et al. Directed evolution of APEX2 for electron microscopy and proximity labeling. Nat Methods 2015;12:51-4.
38. Yang R, Gao W, Wang Z, Jian H, Peng L, Yu X, et al. Polyphyllin I induced ferroptosis to suppress the progression of hepatocellular carcinoma through activation of the mitochondrial dysfunction via Nrf2/HO-1/GPX4 axis. Phytomedicine 2024;122:155135.
39. Goldstein JL, Brown MS. Regulation of the mevalonate pathway. Nature 1990;343:425-30.
40. Jiang W, Hu JW, He XR, Jin WL, He XY. Statins: a repurposed drug to fight cancer. J Exp Clin Cancer Res 2021;40:241.
41. Istvan ES, Deisenhofer J. Structural mechanism for statin inhibition of HMG-CoA reductase. Science 2001;292:1160-4.

Received: 9 April 2026. Accepted: 15 May 2026.

Licensee PAGEPress, Italy
European Journal of Histochemistry 2026; 70:4575
doi:10.4081/ejh.2025.4575